



HAL
open science

A revised parameterization for gaseous dry deposition in air-quality models

L. Zhang, J. R. Brook, R. Vet

► **To cite this version:**

L. Zhang, J. R. Brook, R. Vet. A revised parameterization for gaseous dry deposition in air-quality models. *Atmospheric Chemistry and Physics*, 2003, 3 (6), pp.2067-2082. hal-00295366

HAL Id: hal-00295366

<https://hal.science/hal-00295366>

Submitted on 18 Jun 2008

HAL is a multi-disciplinary open access archive for the deposit and dissemination of scientific research documents, whether they are published or not. The documents may come from teaching and research institutions in France or abroad, or from public or private research centers.

L'archive ouverte pluridisciplinaire **HAL**, est destinée au dépôt et à la diffusion de documents scientifiques de niveau recherche, publiés ou non, émanant des établissements d'enseignement et de recherche français ou étrangers, des laboratoires publics ou privés.

A revised parameterization for gaseous dry deposition in air-quality models

L. Zhang, J. R. Brook, and R. Vet

Meteorological Service of Canada, 4905 Dufferin Street, Toronto, Ontario, M3H 5T4, Canada

Received: 11 March 2003 – Published in Atmos. Chem. Phys. Discuss.: 28 March 2003

Revised: 27 October 2003 – Accepted: 13 November 2003 – Published: 28 November 2003

Abstract. A parameterization scheme for calculating gaseous dry deposition velocities in air-quality models is revised based on recent study results on non-stomatal uptake of O_3 and SO_2 over 5 different vegetation types. Non-stomatal resistance, which includes in-canopy aerodynamic, soil and cuticle resistances, for SO_2 and O_3 is parameterized as a function of friction velocity, relative humidity, leaf area index, and canopy wetness. Non-stomatal resistance for other chemical species is scaled to those of SO_2 and O_3 based on their chemical and physical characteristics. Stomatal resistance is calculated using a two-big-leaf stomatal resistance sub-model for all gaseous species of interest. The improvements in the present model compared to its earlier version include a newly developed non-stomatal resistance formulation, a realistic treatment of cuticle and ground resistance in winter, and the handling of seasonally-dependent input parameters. Model evaluation shows that the revised parameterization can provide more realistic deposition velocities for both O_3 and SO_2 , especially for wet canopies. Example model output shows that the parameterization provides reasonable estimates of dry deposition velocities for different gaseous species, land types and diurnal and seasonal variations. Maximum deposition velocities from model output are close to reported measurement values for different land types. The current parameterization can be easily adopted into different air-quality models that require inclusion of dry deposition processes.

1 Introduction

Dry deposition is an important process that must be addressed in regional air-quality models. Wesely (1989) developed a parameterization scheme for estimating gaseous dry deposition velocities, which has been widely used in a number of models (RADM, Chang et al., 1987; STEM, Carmichael et al., 1991; URM, Harley et al., 1993; CMAQ, Byun and Ching, 1999). Similar dry deposition models have been developed for air-quality models around the world (e.g. Padro et al., 1991; Scire, 1991; Ganzeveld and Leieveld, 1995; Pleim and Xiu, 1995; Zhang et al., 2002a; Wu et al., 2003). Some single layer (usually called big-leaf) and multi-layer dry deposition models have also been developed for estimating acid rain and dry deposition inputs to ecosystems (e.g. Erisman et al., 1994b; Duyzer and Fowler, 1994; Meyers et al., 1998; Brook et al., 1999a; Smith et al., 2000). There are many other models involving dry deposition calculations for specific applications (e.g. Gao et al., 1993; Kramm et al., 1995; Singles et al., 1998; McDonald-Buller et al., 1999; Tetzlaff et al., 2002; A review of available dry deposition models was recently reported by Wesely and Hicks (2000).

Most existing dry deposition models utilize the multiple resistance analogy approach when parameterizing the deposition velocity to vegetation and other surfaces. In this approach, the canopy resistance is usually separated into stomatal and non-stomatal portions. While the overall deposition flux is the major concern of most air-quality models, it can be important to separate the stomatal uptake of pollutants from the overall deposition for some applications (e.g. O_3 dose to agricultural crops, Emberson et al., 2000; Massman et al., 2000). Separating stomatal and non-stomatal uptake leads to more accurate representation of diurnal variations of dry deposition, which is also crucial for air-quality models. Separation of these processes is necessary because stomatal uptake only occurs during the daytime for most canopy types,

Correspondence to: L. Zhang
(leiming.zhang@ec.gc.ca)

during which time it dominates over non-stomatal uptake for many chemical species.

There are many different approaches for stomatal resistance calculations ranging from simple parameterizations as functions of solar radiation and/or time of day (Wesely, 1989; Padro et al., 1991), one- or two-big-leaf approaches (Jarvis, 1976; Hicks et al., 1987; Zhang et al., 2002a), to a multi-layer leaf-resistance model (Baldocchi et al., 1987). For non-stomatal resistance, a constant is typically chosen for a particular season and land type (e.g. Wesely, 1989; Zhang et al., 2002a), thereby ignoring many processes that can effect this deposition pathway. Recent measurements have demonstrated that non-stomatal uptake is affected by meteorological conditions, such as friction velocity (u_*), relative humidity (RH) and canopy wetness, as well as biological factors, such as canopy type, leaf area index (LAI) and growing period. For example, measurements over several different canopies (forests, maize) in France (Lamaud et al., 2002; Laville et al., 2002; Lopez et al., 2002) showed that the non-stomatal uptake of O_3 (i.e. the nighttime deposition) is controlled by the friction velocity. However, to date only a few models have included meteorological information in their non-stomatal formulations, e.g. u_* in the in-canopy aerodynamic resistance and RH in the cuticle resistance (Erisman et al., 1994a, b). Recently, Zhang et al. (2002b, 2003) analyzed O_3 and SO_2 deposition flux data (Zhang et al., 2002b, 2003) from measurements taken over five different canopies (mixed forest, deciduous forest, corn, soybean and pasture) in the eastern USA (Meyers et al., 1998; Finkelstein et al., 2000) and proposed a new set of parameterizations for the non-stomatal resistance including in-canopy, soil and cuticle resistances. These led to better agreement between model results and measurements, thereby demonstrating the value of more detailed treatment of the processes influencing non-stomatal uptake.

The purpose of this study is to develop an improved dry deposition parameterization scheme for air quality models by including the newly developed non-stomatal resistance parameterizations (i.e., Zhang et al., 2002b, 2003). We build upon the model (a big-leaf model) presented in Zhang et al. (2002a), which was developed for calculating dry deposition velocities for 31 gaseous species for AURAMS (Moran et al., 1998), but which only included seasonally-adjusted values for non-stomatal resistance. Other improvements to this previous model include more realistic treatment of cuticle and ground resistance in winter and the handling of seasonally-dependent input parameters.

The new model presented in this paper represents the first attempt of which we are aware to include more realistic non-stomatal uptake parameterizations for a wide range of gaseous compounds. While we show in this paper that this new model improves dry deposition estimates for O_3 and SO_2 and is thus expected to lead to more reliable air quality models, the new model still has many limitations and uncertainties requiring further investigation. For example, the dif-

ferent non-stomatal resistance values used for SO_2 over dew and rain wetted canopies are only based on results from measurements at one site (Zhang et al.; 2003). This is because sufficient SO_2 flux data to estimate the required parameters are very limited. This weakness clearly points to the need for more SO_2 flux data over a wide variety of conditions. Similar data for the other 29 gaseous compounds treated in this present model are scarce if not non-existent. It has therefore been necessary to resort to the approach proposed by Wesely et al. (1989), which is based upon solubility and reactivity, to include these compounds. This will continue to be a weakness of unknown uncertainty in air quality models until significant advances are made in measuring fluxes for many different compounds.

Earlier studies show that aqueous-phase chemistry plays an important role for both O_3 and SO_2 deposition (Fowler et al., 1979; Chamberlain, 1987; Wesely et al., 1990). Though aqueous-phase processes are considered in most air-quality models (in cloud and rain processes) this process cannot be treated explicitly in simple big-leaf dry deposition models due to the unavailability of pollutant concentrations, pH values and other related information at the leaf surface. Thus, uncertainties exist in simple parameterizations like the one presented here, due to variations in the aqueous-phase processes caused by variations in wetness formation mechanisms, geographical locations and many other factors. Other important processes missed in the current model include the co-deposition of SO_2 and NH_3 (Erisman et al., 1993, 1994b; Cape et al., 1998), bi-directional gas exchange or the compensation point (Sorteberg and Hov, 1996; Sutton et al., 1998; Flechard et al., 1999; Husted et al., 2000; Spindler et al., 2001) and the dependence of SO_2 and NH_3 soil resistance on soil pH (Erisman et al., 1994b). Co-deposition of SO_2 and NH_3 is important under wet and humid conditions and bi-directional exchange is important for emitted species. These processes are not included in the present model due to a lack of information over broad land types. Other uncertainties (as discussed in Zhang et al., 2003) include those related to the calculation of the aerodynamic and quasi-laminar resistance, which are not exact representations of the actual processes.

Obviously, errors in the flux measurements from which the model has been developed and tested also contribute to subsequent model uncertainty. Such errors are likely greater under certain conditions (e.g. nighttime stable situations) and vary by location and chemical compound. Furthermore, complete understanding of air-surface exchange processes, especially at the micro-scale, is lacking and thus model formulations and parameterizations are currently relatively simplistic representations of some, if not most, of these processes.

Despite many uncertainties discussed above, a well-developed big-leaf model can lead to flux estimates that are as good as some more sophisticated models (Meyers et al., 1998; Wu et al., 2003), given our present relatively limited

knowledge about all the processes controlling dry deposition. The simpler models also have the advantage of requiring fewer assumptions regarding input parameters, which potentially avoids additional uncertainties.

The land use categories (LUC) used in Zhang et al. (2002a) are based, with some modifications, on BATS (Biosphere Atmosphere Transfer Scheme, Dickinson, 1986). This scheme was generated from 205 global land types with high resolution (1 km × 1 km) satellite data. Cross-references between the original 205 land types of BATS and other schemes (e.g. SiB, Dorman and Sellers, 1989; SiB2, Sellers et al., 1996) are also available. Substantial information on LUC specified parameters (e.g. LAI, roughness length, z_0) are available so this scheme has been widely-used around the world. The LUC of the present work is adopted from the LUC in GEM (Coté et al., 1997), Canada's weather forecast model, and is also based on BATS, plus an extra 6 LUCs.

The next section describes in detail the model formulae. Suggested values for two important input parameters (LAI and z_0) are given in Sect. 3. Comparison of model results with single site measurements of O₃ and SO₂ dry deposition velocity and example model output are given in Sect. 4. The nomenclature of all parameters used in this paper and definitions of 31 gaseous species are listed in an Appendix.

2 Model description

The scheme for the revised model is shown in Fig. 1. The primary resistances to pollutant uptake are the aerodynamic resistance (R_a), the quasi-laminar sublayer resistance (R_b) above the canopy, and the overall canopy resistance (R_c). R_c can be separated into two parallel paths; one is stomatal resistance (R_{st}) with its associated mesophyll resistance (R_m), and the other is non-stomatal resistance (R_{ns}). R_{ns} can be further decomposed into resistance to soil uptake, which includes in-canopy aerodynamic resistance (R_{ac}) and the subsequent soil resistance (R_g), as well as resistance to cuticle uptake (R_{cut}). Note that R_{cut} here is slightly different from that defined in traditional big-leaf models in that it also considers the aerodynamic and quasi-laminar resistances of individual leaves. This is done by parameterizing R_{cut} as a function of friction velocity, similar to the concept of overall cuticle uptake considered in a multi-layer model framework (e.g. Baldocchi, 1988).

Based on the above discussion, the dry deposition velocity, V_d , is defined as:

$$V_d = \frac{1}{R_a + R_b + R_c} \quad (1)$$

where expressions for R_a and R_b can be found in many earlier dry deposition studies (e.g. Erisman et al., 1994b; Massman et al., 1994; Padro et al., 1991; Padro, 1996; Wesely et al., 2001). The uncertainties in R_a and R_b from the different models are small, although large errors can exist under

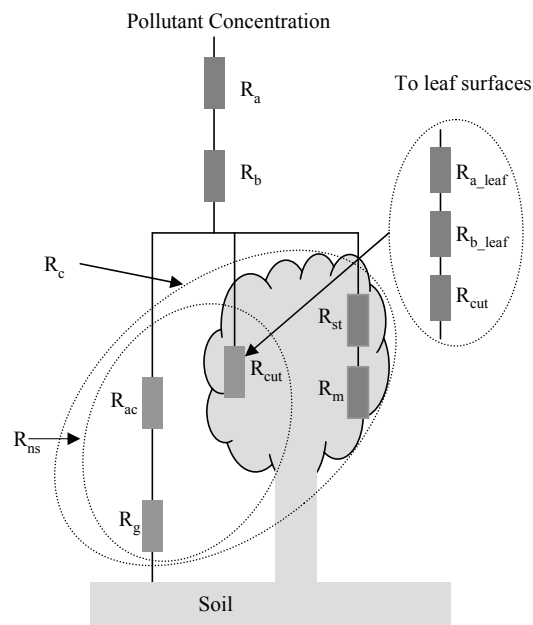


Fig. 1. Scheme of resistance analogy.

strong stable conditions (Massman et al., 1994; Zhang et al., 2003). In the present study, only R_c is discussed. R_c is parameterized as (Zhang et al., 2002b):

$$\frac{1}{R_c} = \frac{1 - W_{st}}{R_{st} + R_m} + \frac{1}{R_{ns}} \quad (2)$$

$$\frac{1}{R_{ns}} = \frac{1}{R_{ac} + R_g} + \frac{1}{R_{cut}} \quad (3)$$

where W_{st} is the fraction of stomatal blocking under wet conditions. R_{st} is calculated using a sunlit/shade (so-called two-big-leaf) stomatal resistance sub-model (Zhang et al., 2002a). R_m is treated as dependent only on the chemical species and we used the values for some common species considered in air-quality models as specified in Zhang et al. (2002a). Note that Eqs. (2) and (3) are for surfaces with canopies. For surfaces without canopies (e.g. water, ice, desert), R_{st} , R_m , R_{ac} and R_{cut} are not applicable. For the convenience of using the same equations for all LUCs, we define R_g as the resistance to any surfaces, e.g. soil, ice, snow and water (more discussion below). Thus, for surfaces without canopies, a value of 0 is given to R_{ac} and a very large value (i.e. 10^{25} s m^{-1}) is used for R_{st} , R_m and R_{cut} . R_{ac} is not chemical species-dependent while R_g and R_{cut} are. R_g and R_{cut} are calculated for SO₂ and O₃ and then scaled for other gaseous species based on the formula (similar to Wesely, 1989):

$$\frac{1}{R_x(i)} = \frac{\alpha(i)}{R_x(\text{SO}_2)} + \frac{\beta(i)}{R_x(\text{O}_3)} \quad (4)$$

where R_x represents non-stomatal resistance components (i.e., R_{cut} and R_g) and i represents the particular gaseous

Table 1. Land use categories and all related parameters (all resistance have a unit of s m^{-1} , na=not applicable; $f(u)$ means a function of wind speed).

LUC	R_{ac0}	R_{cutd0} O ₃	R_{cutw0} O ₃	R_{cutd0} SO ₂	R_{gd} SO ₂	r_{stmin} (s m^{-1})	b_{rs} (W m^{-2})	T_{min} (°C)	T_{max} (°C)	T_{opt} (°C)	b_{vpd} (kPa^{-1})	ψ_{c1} (Mpa)	ψ_{c2} (Mpa)	z_0 (m)	Sd_{max} (cm)
1 water	0	na	na	na	20	na	na	na	na	na	na	na	na	f(u)	na
2 ice	0	na	na	na	Eq. (8a)	na	na	na	na	na	na	na	na	0.01	1
3 inland lake	0	na	na	na	20	na	na	na	na	na	na	na	na	f(u)	na
4 evergreen needleleaf trees	100	4000	200	2000	200	250	44	-5	40	15	0.31	-2	-2.5	0.9	200
5 evergreen broadleaf trees	250	6000	400	2500	100	150	40	0	45	30	0.27	-1	-5.0	2.0	400
6 deciduous needleleaf trees	60–100	4000	200	2000	200	250	44	-5	40	15	0.31	-2	-2.5	0.4–0.9	200
7 deciduous broadleaf trees	100–250	6000	400	2500	200	150	43	0	45	27	0.36	-1.9	-2.5	0.4–1.0	200
8 tropical broadleaf trees	300	6000	400	2500	100	150	40	0	45	30	0.27	-1	-5.0	2.5	400
9 drought deciduous trees	100	8000	400	6000	300	250	44	0	45	25	0.31	-1	-4.0	0.6	200
10 evergreen broadleaf shrubs	60	6000	400	2000	200	150	40	0	45	30	0.27	-2	-4.0	0.2	50
11 deciduous shrubs	20–60	5000	300	2000	200	150	44	-5	40	15	0.27	-2	-4.0	0.05–0.2	50
12 thorn shrubs	40	5000	300	2000	200	250	44	0	45	25	0.27	-2	-3.5	0.2	50
13 short grass and forbs	20	4000	200	1000	200	150	50	5	40	30	0	-1.5	-2.5	0.04	5
14 long grass	10–40	4000	200	1000	200	100	20	5	45	25	0	-1.5	-2.5	0.02–0.1	20
15 crops	10–40	4000	200	1500	200	120	40	5	45	27	0	-1.5	-2.5	0.02–0.1	10
16 rice	10–40	4000	200	1500	50	120	40	5	45	27	0	-1.5	-2.5	0.02–0.1	10
17 sugar	10–40	4000	200	2000	200	120	50	5	45	25	0	-1.5	-2.5	0.02–0.1	10
18 maize	10–50	5000	300	2000	200	250	65	5	45	25	0	-1.5	-2.5	0.02–0.1	10
19 cotton	10–40	5000	300	2000	200	125	65	10	45	30	0	-1.5	-2.5	0.02–0.2	10
20 irrigated crops	20	4000	200	2000	50	150	40	5	45	25	0	-1.5	-2.5	0.05	10
21 urban	40	6000	400	4000	300	200	42	0	45	22	0.31	-1.5	-3	1.0	50
22 tundra	0	8000	400	2000	300	150	25	-5	40	20	0.24	0	-1.5	0.03	2
23 swamp	20	5000	300	1500	50	150	40	0	45	20	0.27	-1.5	-2.5	0.1	10
24 Desert	0	na	na	na	700	na	na	na	na	na	na	na	na	0.04	2
25 mixed wood forests	100	4000	200	2500	200	150	44	-3	42	21	0.34	-2	-2.5	0.6–0.9	200
26 Transitional forest	100	4000	200	2500	200	150	43	0	45	25	0.31	-2	-3	0.6–0.9	200

species. Parameters α and β are two scaling factors based on the chemical species' solubility and half-redox reactivity (Wesely, 1989). Scaling parameters for a total of 31 species are presented in Table 1 of Zhang et al. (2002a). The details of each of the terms in Eqs. (2)–(4) are discussed below.

W_{st} : Zhang et al. (2002b), using O₃ flux data from five sites in eastern North America, found that W_{st} is not important under most wet conditions because of weak solar radiation (SR), which leads to large R_{st} . However, there are some exceptions to this such as morning dew and sunshine immediately after rain when solar radiation is strong. In such cases, we calculate a small R_{st} (see Eq. 6), however, stomata can be partially blocked by water films and the W_{st} term will then increase the stomatal resistance. Thus, the following formula is suggested for wet canopies (for dry canopies, W_{st} always equals 0):

$$W_{st} = \begin{cases} 0, & SR \leq 200 \text{ W m}^{-2} \\ (SR - 200)/800, & 200 < SR \leq 600 \text{ W m}^{-2} \\ 0.5, & SR > 600 \text{ W m}^{-2} \end{cases} \quad (5)$$

W_{st} is given a value other than 0 only when solar radiation is relatively strong ($>200 \text{ W m}^{-2}$) and the canopy is wet. If

rain or dew occurs, the canopy is treated as wet. The occurrence of dew is defined based on particular meteorological conditions, e.g. RH, u_* and cloud cover (Janssen and Romer, 1991) as adopted in Brook et al. (1999a). Note that Wesely (1989) increased the stomatal resistance by a factor of 3 (equivalent of a W_{st} of 0.67) for wet surfaces. Zhang et al. (2002a) used several constants for different wet conditions (0.7 for dew and 0.9 for rain). Our data show that these values are probably too large for most wet conditions and thus the new formula is suggested with an upper limit of 0.5 for W_{st} .

R_{st} : The following sunlit/shade stomatal resistance sub-model (Zhang et al., 2002a) is used for calculating R_{st} for all gaseous species:

$$R_{st} = 1/[G_s(PAR)f(T)f(D)f(\psi)D_i/D_v] \quad (6)$$

where $G_s(PAR)$ is the unstressed leaf stomatal conductance, a function of photosynthetically active radiation (PAR). Calculation of $G_s(PAR)$ is described in Zhang et al. (2002a) and is not repeated here. The dimensionless functions $f(T)$, $f(D)$ and $f(\psi)$ represent the conductance-reducing effects of air temperature T , water-vapour-pressure deficit D , and water stress (leaf water potential) ψ , respectively, on leaf

stomatal conductance (Brook et al., 1999a). The formulas for these functions are:

$$f(T) = \frac{T - T_{min}}{T_{opt} - T_{min}} \left[\frac{T_{max} - T}{T_{max} - T_{opt}} \right]^{b_t} \quad (6a)$$

with

$$b_t = \frac{T_{max} - T_{opt}}{T_{opt} - T_{min}} \quad (6b)$$

$$f(D) = 1 - b_{vpd} D \quad (6c)$$

with

$$D = e^*(T) - e \quad (6d)$$

and

$$f(\psi) = (\psi - \psi_{c2}) / (\psi_{c1} - \psi_{c2}) \quad (6e)$$

with

$$\psi = -0.72 - 0.0013 SR \quad (6f)$$

T_{min} and T_{max} are minimum and maximum temperatures (°C) that indicate the temperatures below and above which complete stomatal closure occurs. T_{opt} is an optimum temperature that indicates the temperature of maximum stomatal opening. b_{vpd} is a water-vapour-pressure-deficit constant (kPa^{-1}), D is the vapour pressure deficit (kPa), $e^*(T)$ is the saturation water vapour pressure (kPa) at air temperature T (°C), and e is the ambient water vapour pressure (kPa). ψ_{c1} and ψ_{c2} (MPa) are parameters that specify leaf-water-potential dependency. When $\psi > \psi_{c1}$ (i.e. no leaf water potential stress), $f(\psi)=1.0$. Values for all parameters required for calculating R_{st} are taken from Brook et al. (1999a), Dorman and Sellers (1989), Dickinson et al. (1986), and NOAA (1992) library data, and are listed in Table 1. These parameters are r_{smin} (minimum stomatal resistance), b_{rs} (empirical light response coefficient), T_{min} , T_{max} , T_{opt} , b_{vpd} , ψ_{c1} and ψ_{c2} . Explicitly consideration of the soil moisture content in $f(\psi)$ as was done in Wesely et al. (2001) is preferable, however, LUC-specific parameters for the soil moisture effect on R_{st} are very limited. Therefore an approach, which follows Sellers et al. (1996), is used as we have in the past (Brook et al., 1999a).

During nighttime when there is no solar radiation, the leaf stomata are assumed to be completely closed. R_{st} estimated from Eq. (6) then has an infinite value. Recent research suggests that the stomata of some canopy species may still be partially open even at night (Gunthardt-Goerg et al., 1997; Musselman and Minnick, 2000; Wisner and Havranek, 1993, 1995). However, this behaviour is difficult to quantify given present knowledge. In this study we treat the stomata as fully closed at night.

R_{ac} : In-canopy aerodynamic resistance should be the same for all gaseous species. The formula developed in Zhang et al. (2002b) is used:

$$R_{ac} = \frac{R_{ac0} LAI^{1/4}}{u_*^2} \quad (7)$$

where R_{ac0} is the reference value for in-canopy aerodynamic resistance. R_{ac0} is expected to vary with different canopy types and suggested values are given in Table 1 for all LUCs. For some LUCs, a range of R_{ac0} values is given to reflect the change of canopy structure at different times of the growing season. The minimum values, $R_{ac0}(min)$, correspond to leafless periods for deciduous forests and earlier growing periods for agricultural lands. The maximum values, $R_{ac0}(max)$, correspond to the full-leaf period for forests and the maturity period for agricultural lands. Here, a simple formula is suggested for extracting R_{ac0} values for any day of the year based on minimum and maximum LAI values since this information is available in most air-quality models:

$$R_{ac0}(t) = R_{ac0}(min) + \frac{LAI(t) - LAI(min)}{LAI(max) - LAI(min)} \times [R_{ac0}(max) - R_{ac0}(min)] \quad (7a)$$

where $R_{ac0}(t)$ corresponds to the R_{ac0} value at any day of the year. $LAI(min)$ and $LAI(max)$ represents minimum and maximum LAI values, respectively, during the year.

Wesely (1989) specified a constant in-canopy aerodynamic resistance for forest canopies and Erisman et al. (1994b) suggested a formula as a function of canopy height and friction velocity. In the present study, canopy height is not included since its effect is implicitly included in the friction velocity and, more importantly, in the reference values of R_{ac0} . As can be seen from Table 1, R_{ac0} is larger for tall canopies than for short canopies and this is consistent with Erisman et al. (1994b).

R_g : Ground resistance is considered separately for different surface types (water, ice, snow, soil). The following equation is used according to Erisman et al. (1994b):

$$R_g = \begin{cases} R_{water} \\ R_{ice} \\ R_{snow} \\ R_{soil} \end{cases} \quad (8)$$

where R_{water} , R_{ice} , R_{snow} and R_{soil} represent resistance to water, ice, snow, and soil surfaces, respectively. R_{snow} and R_{ice} are assumed to have the same values. For O_3 , R_{water} , R_{snow} and R_{ice} are given a value of 2000 s m^{-1} . For SO_2 , R_{water} is given a value of 20 s m^{-1} , while R_{snow} and R_{ice} are taken as a function of temperature with a lower limit of 100 s m^{-1} and an upper limit of 500 s m^{-1} (Erisman et al., 1994b) as follows:

$$R_{snow}, R_{ice}(SO_2) = 70(2 - T) \quad (8a)$$

Information on R_{soil} is limited for both O_3 and SO_2 . Some discussion on soil resistance for SO_2 , O_3 and several NO_y species can be found in Erisman et al. (1994b). O_3 uptake by soils is probably controlled by soil organic material (enhancing the removal) and soil moisture (inhibiting uptake by covering the reaction sites and reducing gas transfer). Based on previous studies and a review of published measurements

(Erisman et al., 1994b; Brook et al., 1999b; Wesely and Hicks, 2000), a value of 200 s m^{-1} is given for O_3 for all vegetated surfaces (LUC 4-19, 25 and 26) and 500 s m^{-1} for non-vegetated surfaces or surfaces with wet ground (LUC 20-24). R_{soil} is more complicated for SO_2 due to its sensitivity to wetness, dependence on soil pH and co-deposition with NH_3 (Erisman and Wyers, 1993; Erisman et al., 1994b). Soil resistance to SO_2 is usually smaller when the surface is wet, and probably different for dew- and rain-wetted surfaces, due to the different aqueous-phase chemistry involved with dew and rain (Zhang et al., 2003). The following approach is suggested for R_{soil} for SO_2 :

$$R_g = \begin{cases} R_{gd} \\ R_{grain} \\ R_{gdew} \end{cases} \quad (8b)$$

where R_{gd} represents the soil resistance over land surfaces where no dew or rain has occurred, R_{grain} and R_{gdew} are the resistances to soil when rain or dew has occurred. Values of 50 and 100 s m^{-1} are assigned to R_{grain} and R_{gdew} , respectively. Suggested R_{gd} values for all LUCs are presented in Table 1. For canopies with relatively high soil moisture content (e.g. tropical forest), R_{gd} is given a smaller value compared to vegetation types with dry soils (e.g. desert). Note that soil pH and moisture content are not explicitly considered in the present study.

R_{cut} : Canopy cuticle resistance is calculated for dry and wet conditions separately according to Zhang et al. (2002b):

$$R_{\text{cutd}} = \frac{R_{\text{cutd0}}}{e^{0.03RH} LAI^{1/4} u_*} \quad (9a)$$

$$R_{\text{cutw}} = \frac{R_{\text{cutw0}}}{LAI^{1/2} u_*} \quad (9b)$$

where RH is relative humidity (in percentage). R_{cutd0} and R_{cutw0} are reference values for dry and wet cuticle resistance, respectively. Values of R_{cutd0} and R_{cutw0} for O_3 and values of R_{cutd0} for SO_2 for each LUC are presented in Table 1. R_{cutw0} for SO_2 is treated differently under dew and rain conditions. For all vegetated surfaces, values of 50 s m^{-1} and 100 s m^{-1} are given for R_{cutw0} for rain and dew conditions, respectively. Equations (9a) and (9b) were developed based on the 5-site flux data set for which u_* values seldom exceeded 1.5 m s^{-1} for the two forest locations and 0.8 m s^{-1} for the other three sites (crops). It is expected that these equations give reasonable values for most conditions, but they may give unrealistically small values for SO_2 when u_* is extremely large (e.g. $u_* > 2 \text{ m s}^{-1}$). Thus, a lower limit of 100 s m^{-1} is suggested for dry canopies and 20 s m^{-1} for wet canopies for SO_2 . Note that Erisman et al. (1994a) first proposed modelling cuticle resistance as a function of RH for SO_2 , and similar chemical species, over dry canopies.

In winter, when temperatures are below -1°C , R_{gd} and R_{cutd} are increased by as much as two times (with an upper

limit of 2 for the term $e^{0.2(-1-T)}$ shown below) their original value according to the formula (similar to Wesely, 1989; Erisman et al., 1994b):

$$R_{gd}(T < -1^\circ\text{C}) = R_{gd} e^{0.2(-1-T)} \quad (10a)$$

$$R_{\text{cutd}}(T < -1^\circ\text{C}) = R_{\text{cutd}} e^{0.2(-1-T)} \quad (10b)$$

For snow on the ground and leaves, both R_g and R_{cut} are adjusted by including a snow cover fraction (f_{snow}):

$$\frac{1}{R_g} = \frac{1 - 2f_{\text{snow}}}{R_g} + \frac{2f_{\text{snow}}}{R_{\text{snow}}} \quad (10c)$$

$$\frac{1}{R_{\text{cut}}} = \frac{1 - f_{\text{snow}}}{R_{\text{cut}}} + \frac{f_{\text{snow}}}{R_{\text{snow}}} \quad (10d)$$

Since snow on ground persists longer than on leaves for high canopies, the snow fraction for the ground (R_g) is taken as 2 times that of leaves (R_{cut}). Note that both f_{snow} and $2f_{\text{snow}}$ have a range of values between 0.0–1.0. Though the snow fraction might be available in some meteorological models, it represents a grid-averaged value, which probably does not represent the snow cover of canopy leaves and underlying surfaces. Considering the limited knowledge at present stage, we suggested a simple formula to estimate f_{snow} from snow depth (sd in cm) similar to the approach used in climate models:

$$f_{\text{snow}} = \frac{sd}{sd_{\text{max}}} \quad (10e)$$

where sd_{max} is a parameter at or above which value the snow fraction for canopy leaves is assumed to be 1. Suggested sd_{max} values are also listed in Table 1 (Note that the actual sd_{max} for underlying soil surfaces is only half of the values presented in Table 1 as can be seen from the comparison of Eqs. (10c) and (10d)).

3 Other parameters

LAI is an important parameter for calculating canopy resistances. LAI values used in GEM are adopted here. Monthly LAI values at the beginning of each month are presented in Fig. 2. LAI values on any day are interpolated using the day number of the month. Note that several LUCs that have constant LAI values are not shown in Fig. 2. They are set to 5.0 (LUC 4), 6.0 (LUC 5, 8), 4.0 (LUC 9, 23), 3.0 (LUC 10, 12), 1.0 (LUC 13) and 0.0 (LUC 1-3, 22, 24). LAI values for LUC 21 (urban) are set to a constant value of 1 in GEM. Since LAI values for urban locations in different regions can have quite different seasonal variations, we chose to assign a value of 0.1 in the winter season, gradually increasing to 1 in the late spring. We keep it as 1 until early fall, and then reduce it gradually to 0.1 again at the end of fall (figure not shown).

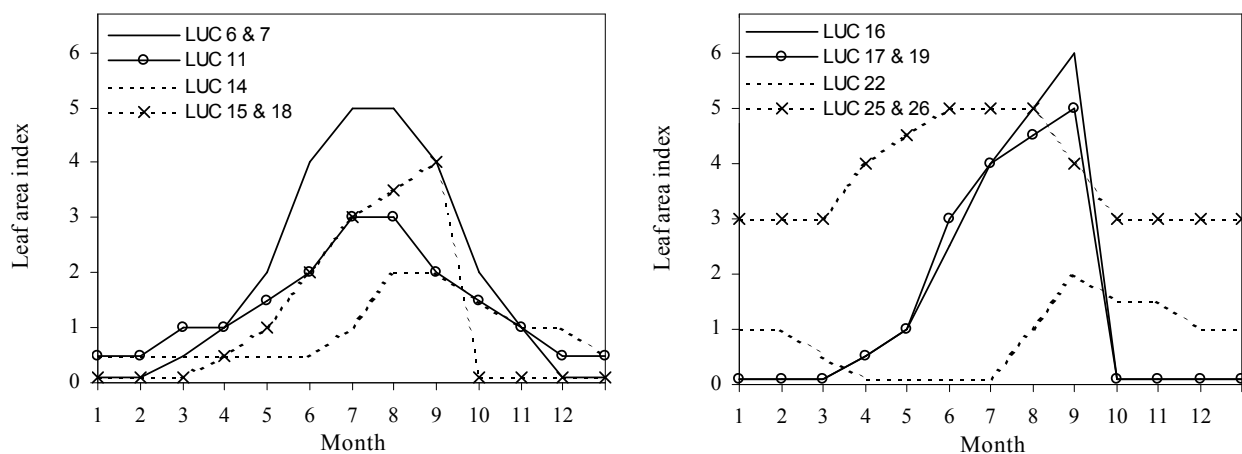


Fig. 2. Leaf area index in the Northern Hemisphere.

Roughness length (z_0) is needed for calculating friction velocity, which subsequently affects aerodynamic, quasi-laminar and non-stomatal resistances. z_0 from GEM cannot be used directly since it is treated together with topography. Dorman and Sellers (1989) presented monthly z_0 for many different land types. Panofsky and Dutton (1984) and Pielke (1984) also reviewed typical z_0 values for different land types. Based on these studies, z_0 values for each LUC are suggested and presented in Table 1. For water surfaces (LUC 1 and 3), z_0 is calculated as a function of wind speed or friction velocity (e.g. Hicks and Liss, 1976). For some surfaces a constant z_0 value is suggested, while for others a range of z_0 values is given. For those surfaces that have variable z_0 values, a formula similar to Eq. (7a) is used to obtain z_0 for any time period based on LAI values:

$$z_0(t) = z_0(\min) + \frac{LAI(t) - LAI(\min)}{LAI(\max) - LAI(\min)} \times [z_0(\max) - z_0(\min)] \quad (11)$$

4 Model evaluation and example output

4.1 Comparison with measurements

The major improvement of the present model is in the non-stomatal resistance parameterization, especially for wet canopies. Thus, we chose the measurements of O_3 and SO_2 dry deposition data at the Kane site (deciduous forest in Pennsylvania, lat: 41.595° N, long: 78.766° W, USA; 29 April to 23 October 1997; Finkelstein et al., 2000). This is the only site that has a sufficiently large data set for O_3 and SO_2 under wet canopy conditions to allow a thorough test of the performance of the revised model. Measured meteorological data (u_* , stability, solar radiation and wetness) and biological (LAI) information are used in calculating dry deposition velocities. To show the improvements of the present model compared to its earlier version (Zhang et al., 2002a),

results from both model versions for the mean diurnal cycle of half-hourly V_d over wet canopies, along with the observations, are presented in Figs. 3b and d. For dry canopies, only results from the present model are shown in Figs. 3a and c since the differences between the present and the previous model diurnal average results are small because the same stomatal resistance sub-model is used in both models.

The suitability of the present model can be seen from the agreement of modelled O_3 and SO_2 deposition velocity compared to the observations for both dry and wet canopies and the improved results compared to its previous version for wet canopies. It should be pointed out that the previous version already considered, to some extent, dew and rain effects on cuticle uptake based on the knowledge at the time the model was developed. For example, a constant cuticle resistance of 400 $s\ m^{-1}$ and 800 $s\ m^{-1}$ was used for O_3 under rain and dew conditions, respectively, and 100 $s\ m^{-1}$ and 200 $s\ m^{-1}$ for SO_2 under rain and dew conditions, respectively (Zhang et al., 2002a). However, this model did not agree well with observations (Figs. 3c and d). It overpredicts O_3 V_d during nighttime and underestimates O_3 V_d during the day. The new version captures the higher daily values and also maintains the lower nighttime V_d values. The previous version seems to predict reasonable SO_2 V_d during the night, but underestimates SO_2 V_d during the day. It can be expected that other models, which do not adequately treat dew and rain, will exhibit even less diurnal variations than the results shown here.

Sensitivity tests show that the aerodynamic resistance alone can only explain a small portion of observed diurnal variations over wet canopies, i.e. 20–40% for O_3 , 20–50% for SO_2 , depending on the magnitude of the cuticle and soil resistances (non-stomatal resistance). The larger the non-stomatal resistance, the smaller the diurnal variation caused by aerodynamic resistance variation. Figure 3b, which shows daytime wet canopy conditions, assuming that stomatal uptake is not important for wet canopies in light of stomata blocking by water drops and the presence of very

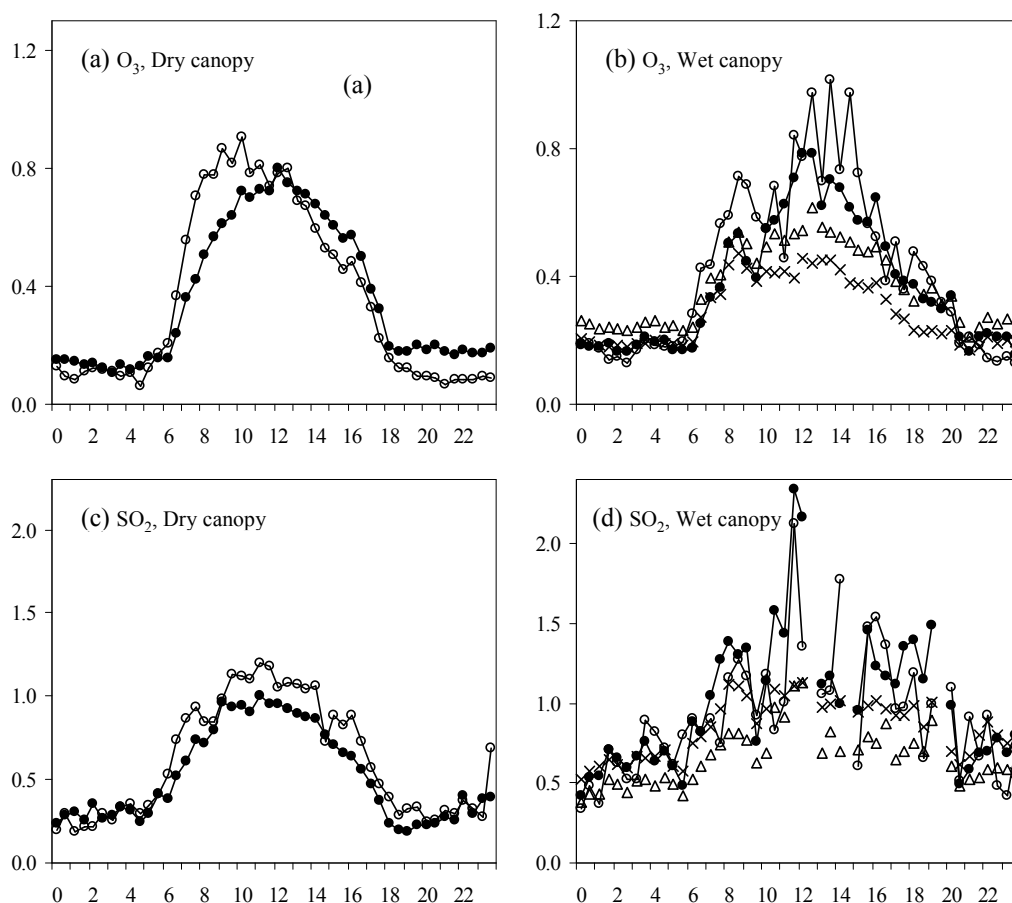


Fig. 3. Average diurnal cycle deposition velocity (cm s^{-1}) from observations (open circle), current model (filled circle), previous model (triangle) and from an assumption of constant cuticle resistance for wet canopies (“x” symbol).

weak solar radiation, indicates that use of a constant value of 400 s m^{-1} for non-stomatal resistance for O_3 results in a good estimation for nighttime O_3 V_d ($\sim 0.2 \text{ cm s}^{-1}$). Then the model predicts a V_d value of 0.45 cm s^{-1} in the early afternoon, which is much smaller than observed value at that time ($0.8\text{--}1.0 \text{ cm s}^{-1}$) (Note that the stomatal resistances are the same for all tests). This demonstrates that aerodynamic resistance alone cannot explain the observed diurnal variations. Thus earlier models fail to predict the correct diurnal cycle when cuticle uptake is not treated as a function of meteorological conditions. Similar conclusions can be drawn for SO_2 except that the aerodynamic resistance can cause slightly larger diurnal variations compared to O_3 because of the very small non-stomatal resistance used for SO_2 over wet canopies. For example (Fig. 3d), a constant non-stomatal resistance of 80 s m^{-1} produces reasonable nighttime SO_2 V_d ($0.5\text{--}0.8 \text{ cm s}^{-1}$ compared to observations $0.4\text{--}0.8 \text{ cm s}^{-1}$). The highest daytime SO_2 V_d value predicted is 1.2 cm s^{-1} (note that the inverse of 80 s m^{-1} is around 1.2 cm s^{-1}), which is still smaller than observed values ($>2 \text{ cm s}^{-1}$). Only when meteorological influences are

explicitly included in the non-stomatal resistance (i.e. the present model), can the observed SO_2 V_d values be reproduced.

As mentioned above, the conclusions are based on the assumption that stomatal uptake is not important for wet canopies in light of stomata blocking by water drops and the presence of very weak solar radiation, which controls stomata opening. This assumption is consistent with limited earlier studies (e.g. Fuentes et al., 1992; Grantz et al., 1995). Ultimately, this assumption is best verified using CO_2 and H_2O flux data over wet canopies. However, CO_2 and H_2O flux data at this site and the other sites we have used previously are not available. Thus further studies are still needed to verify this assumption.

4.2 Modelled maximum V_d values for dry and wet canopies

Based upon the model structure described above we expect model results to be sensitive to several of the input parameters, namely LAI , z_0 , u_* , SR , T and RH . These parameters can vary widely due to meteorological variations (i.e. hourly to daily) and seasonal variations, as well as

Table 2. Predicted maximum dry deposition velocity (cm s^{-1}) for dry (left column) and wet (right column) canopies for 31 chemical species. A value of 0.0 (over water or ice surfaces) for some species represents a value smaller than 0.04. Definition of 31 species is listed in the appendix.

LUC	SO ₂	H ₂ SO ₄	NO ₂	O ₃	H ₂ O ₂	HNO ₃	HONO	HNO ₄	NH ₃	PAN	PPN	APAN	MPAN	HCHO	MCHO	PALD
1	2.1,2.1	2.0,2.0	0.0,0.0	0.1,0.1	2.1,2.1	2.6,2.6	2.7,2.7	2.6,2.6	2.2,2.2	0.0,0.0	0.0,0.0	0.0,0.0	0.0,0.0	1.9,1.9	0.0,0.0	0.0,0.0
2	0.8,0.8	0.8,0.8	0.0,0.0	0.1,0.1	0.9,0.9	3.0,3.0	1.4,1.4	2.3,2.3	0.8,0.8	0.0,0.0	0.0,0.0	0.0,0.0	0.0,0.0	0.7,0.7	0.0,0.0	0.0,0.0
3	2.1,2.1	2.0,2.0	0.0,0.0	0.1,0.1	2.1,2.1	2.6,2.6	2.7,2.7	2.6,2.6	2.2,2.2	0.0,0.0	0.0,0.0	0.0,0.0	0.0,0.0	1.9,1.9	0.0,0.0	0.0,0.0
4	1.5,3.8	2.0,4.1	1.2,1.5	1.3,1.7	2.2,4.4	5.1,5.1	3.1,5.2	4.8,5.0	1.9,4.1	0.9,1.1	0.9,1.1	0.9,1.3	0.6,0.7	1.7,3.6	0.4,0.3	0.4,0.3
5	1.7,3.9	2.0,4.1	1.2,1.3	1.3,1.4	2.2,4.4	5.3,5.3	3.1,5.4	4.8,5.3	2.1,4.2	0.9,0.9	0.9,0.9	0.9,1.1	0.7,0.6	1.8,3.7	0.5,0.4	0.4,0.3
6	1.5,3.8	2.0,4.1	1.2,1.5	1.3,1.7	2.2,4.4	5.1,5.1	3.1,5.2	4.8,5.0	1.9,4.1	0.9,1.1	0.9,1.1	0.9,1.3	0.6,0.7	1.7,3.6	0.4,0.3	0.4,0.3
7	1.5,3.7	1.8,3.8	1.2,1.1	1.2,1.2	2.0,4.1	5.1,5.1	2.8,5.2	4.3,5.0	2.0,4.0	0.8,0.8	0.8,0.8	0.9,0.9	0.6,0.5	1.7,3.5	0.5,0.3	0.4,0.3
8	1.7,3.8	2.0,4.1	1.2,1.3	1.3,1.4	2.2,4.4	5.3,5.3	3.1,5.4	4.8,5.3	2.1,4.2	0.9,0.9	0.9,0.9	0.9,1.1	0.6,0.6	1.8,3.6	0.5,0.4	0.4,0.3
9	0.9,3.6	1.2,3.8	0.8,0.9	0.9,1.1	1.3,4.0	4.3,5.0	1.9,5.1	3.0,4.9	1.1,3.9	0.6,0.7	0.6,0.7	0.6,0.8	0.4,0.4	1.0,3.4	0.3,0.3	0.3,0.2
10	1.2,2.3	1.4,2.3	0.9,0.8	1.0,0.9	1.6,2.5	3.7,3.7	2.0,3.3	2.8,3.6	1.6,2.5	0.7,0.6	0.7,0.6	0.7,0.7	0.5,0.4	1.3,2.2	0.4,0.3	0.4,0.3
11	1.3,2.3	1.4,2.4	1.0,0.9	1.1,1.0	1.7,2.6	3.7,3.7	2.1,3.4	2.9,3.6	1.7,2.5	0.8,0.7	0.7,0.7	0.8,0.8	0.6,0.5	1.4,2.2	0.4,0.3	0.4,0.3
12	1.1,2.3	1.4,2.4	0.8,0.8	0.9,0.9	1.5,2.6	3.7,3.7	2.0,3.4	2.9,3.6	1.3,2.5	0.6,0.6	0.6,0.6	0.6,0.7	0.4,0.4	1.2,2.2	0.3,0.2	0.3,0.2
13	1.3,1.9	1.5,2.0	0.8,0.8	0.8,0.9	1.6,2.1	3.3,3.3	2.2,2.8	3.0,3.2	1.4,2.0	0.6,0.6	0.6,0.6	0.6,0.7	0.4,0.4	1.3,1.8	0.3,0.2	0.3,0.2
14	1.6,2.2	1.8,2.3	1.3,1.3	1.4,1.3	2.1,2.6	3.5,3.5	2.5,3.2	3.2,3.4	2.1,2.6	1.0,0.9	0.9,0.9	0.9,1.0	0.8,0.7	1.8,2.3	0.5,0.5	0.5,0.4
15	1.6,2.5	1.8,2.6	1.3,1.3	1.4,1.4	2.0,2.8	3.5,3.5	2.5,3.5	3.2,3.4	2.1,2.8	1.0,0.9	0.9,0.9	1.0,1.0	0.8,0.7	1.8,2.5	0.5,0.4	0.5,0.4
16	1.8,2.6	1.9,2.8	1.4,1.4	1.5,1.5	2.2,3.0	3.5,3.5	2.6,3.6	3.3,3.4	2.3,3.0	1.0,1.0	1.0,1.0	1.0,1.1	0.8,0.7	2.0,2.6	0.6,0.4	0.5,0.4
17	1.5,2.5	1.7,2.7	1.3,1.3	1.4,1.4	2.0,2.9	3.5,3.5	2.4,3.6	3.1,3.4	2.0,2.8	1.0,1.0	0.9,0.9	1.0,1.1	0.8,0.7	1.7,2.5	0.5,0.4	0.5,0.4
18	1.1,2.3	1.3,2.4	0.8,0.8	0.9,0.9	1.5,2.6	3.5,3.5	2.0,3.3	2.8,3.4	1.4,2.5	0.6,0.6	0.6,0.6	0.6,0.7	0.4,0.4	1.2,2.2	0.3,0.2	0.3,0.2
19	1.4,2.6	1.6,2.7	1.1,1.0	1.2,1.1	1.8,2.9	3.7,3.7	2.3,3.7	3.1,3.6	1.8,2.9	0.8,0.8	0.8,0.8	0.8,0.9	0.6,0.5	1.5,2.5	0.5,0.3	0.4,0.3
20	1.5,1.9	1.6,2.0	0.6,0.6	0.7,0.7	1.7,2.2	3.3,3.3	2.2,2.8	2.8,3.3	1.6,2.1	0.5,0.5	0.4,0.5	0.5,0.5	0.3,0.3	1.5,1.8	0.3,0.2	0.3,0.2
21	0.8,2.8	1.1,2.9	0.6,0.5	0.6,0.6	1.2,3.1	4.7,5.1	1.9,4.4	3.3,5.0	1.0,3.0	0.4,0.4	0.4,0.4	0.5,0.5	0.3,0.2	0.9,2.6	0.2,0.2	0.2,0.2
22	0.9,2.3	1.1,2.3	0.4,0.5	0.4,0.5	1.1,2.5	3.2,3.2	1.7,3.2	2.7,3.2	0.9,2.4	0.3,0.3	0.3,0.3	0.3,0.4	0.2,0.2	0.8,2.1	0.1,0.2	0.1,0.1
23	1.8,2.5	1.9,2.6	1.0,0.9	1.0,1.0	2.1,2.8	3.5,3.5	2.6,3.5	3.3,3.4	2.2,2.8	0.7,0.7	0.7,0.7	0.7,0.7	0.6,0.5	1.9,2.5	0.4,0.3	0.4,0.3
24	0.2,1.4	0.3,1.5	0.2,0.2	0.2,0.2	0.3,1.5	2.0,3.3	0.6,2.3	1.3,3.2	0.1,1.5	0.1,0.1	0.1,0.1	0.2,0.2	0.1,0.1	0.2,1.3	0.0,0.0	0.0,0.0
25	1.7,3.8	2.0,4.2	1.4,1.6	1.5,1.8	2.3,4.5	5.1,5.1	3.2,5.2	4.7,5.0	2.2,4.2	1.0,1.2	1.0,1.2	1.1,1.4	0.8,0.8	1.9,3.7	0.5,0.4	0.5,0.4
26	1.7,3.8	2.0,4.2	1.4,1.6	1.5,1.8	2.3,4.5	5.1,5.1	3.2,5.2	4.7,5.0	2.1,4.2	1.0,1.2	1.0,1.2	1.1,1.4	0.8,0.7	1.9,3.7	0.5,0.4	0.5,0.4
C4A	C7A	ACHO	MVK	MACR	MGLY	MOH	ETOH	POH	CRES	FORM	ACAC	ROOH	ONIT	INIT		
1	0.0,0.0	0.0,0.0	0.0,0.0	0.0,0.0	0.0,0.0	0.1,0.1	1.7,1.7	1.6,1.6	1.3,1.3	0.1,0.1	2.7,2.7	2.4,2.4	0.5,0.5	0.0,0.0	0.0,0.0	
2	0.0,0.0	0.0,0.0	0.0,0.0	0.0,0.0	0.0,0.0	0.0,0.0	0.5,0.5	0.5,0.5	0.4,0.4	0.0,0.0	1.4,1.4	1.1,1.1	0.1,0.1	0.0,0.0	0.0,0.0	
3	0.0,0.0	0.0,0.0	0.0,0.0	0.0,0.0	0.0,0.0	0.1,0.1	1.7,1.7	1.6,1.6	1.3,1.3	0.1,0.1	2.7,2.7	2.4,2.4	0.5,0.5	0.0,0.0	0.0,0.0	
4	0.4,0.3	0.3,0.2	0.3,0.3	0.5,0.3	0.4,0.3	0.5,0.3	1.4,3.0	1.3,2.8	1.0,2.2	0.4,0.3	2.4,5.2	2.0,4.7	1.3,1.9	0.7,1.0	0.7,0.9	
5	0.4,0.3	0.3,0.3	0.4,0.3	0.6,0.4	0.4,0.3	0.6,0.4	1.6,3.0	1.4,2.9	1.1,2.2	0.5,0.4	2.5,5.4	2.1,4.8	1.3,1.7	0.7,0.8	0.7,0.8	
6	0.4,0.3	0.3,0.2	0.3,0.3	0.5,0.3	0.4,0.3	0.5,0.3	1.4,3.0	1.3,2.8	1.0,2.2	0.4,0.3	2.4,5.2	2.0,4.7	1.3,1.9	0.7,1.0	0.7,0.9	
7	0.4,0.3	0.4,0.3	0.4,0.3	0.7,0.4	0.4,0.3	0.6,0.4	1.5,2.9	1.3,2.8	1.1,2.1	0.5,0.4	2.3,5.2	1.9,4.6	1.2,1.5	0.7,0.7	0.6,0.6	
8	0.4,0.3	0.3,0.3	0.4,0.3	0.6,0.4	0.4,0.3	0.6,0.4	1.6,3.0	1.4,2.9	1.1,2.2	0.5,0.4	2.5,5.4	2.1,4.8	1.3,1.7	0.7,0.8	0.7,0.8	
9	0.3,0.2	0.2,0.2	0.2,0.2	0.3,0.3	0.3,0.2	0.3,0.3	0.8,2.8	0.7,2.7	0.6,2.1	0.3,0.2	1.3,5.1	1.1,4.5	0.8,1.4	0.5,0.6	0.5,0.6	
10	0.4,0.3	0.3,0.2	0.3,0.2	0.5,0.3	0.4,0.3	0.5,0.3	1.2,1.9	1.1,1.8	0.9,1.4	0.4,0.3	1.8,3.2	1.5,2.8	1.0,1.1	0.6,0.5	0.5,0.5	
11	0.4,0.3	0.3,0.3	0.4,0.3	0.6,0.4	0.4,0.3	0.6,0.4	1.3,1.9	1.1,1.8	0.9,1.5	0.5,0.3	1.8,3.2	1.5,2.8	1.1,1.2	0.6,0.6	0.6,0.6	
12	0.3,0.2	0.2,0.2	0.3,0.2	0.3,0.2	0.3,0.2	0.3,0.2	1.0,1.9	0.9,1.8	0.7,1.4	0.3,0.2	1.7,3.2	1.4,2.8	0.9,1.1	0.5,0.5	0.5,0.5	
13	0.2,0.2	0.2,0.2	0.2,0.2	0.3,0.2	0.2,0.2	0.3,0.2	1.0,1.5	1.0,1.5	0.7,1.1	0.2,0.2	1.9,2.5	1.6,2.2	0.8,1.0	0.5,0.5	0.5,0.5	
14	0.5,0.4	0.4,0.4	0.4,0.4	0.8,0.7	0.5,0.4	0.8,0.6	1.6,2.0	1.5,1.9	1.2,1.5	0.7,0.6	2.2,3.0	1.9,2.6	1.4,1.4	0.7,0.8	0.7,0.7	
15	0.5,0.4	0.4,0.3	0.4,0.3	0.8,0.6	0.5,0.4	0.8,0.6	1.6,2.2	1.4,2.0	1.2,1.6	0.7,0.5	2.2,3.3	1.9,2.9	1.4,1.5	0.7,0.8	0.7,0.8	
16	0.5,0.4	0.4,0.4	0.5,0.4	0.9,0.6	0.5,0.4	0.9,0.6	1.8,2.3	1.7,2.2	1.5,1.8	0.8,0.5	2.4,3.5	2.1,3.1	1.5,1.6	0.8,0.9	0.7,0.8	
17	0.5,0.4	0.4,0.3	0.4,0.3	0.8,0.6	0.5,0.4	0.8,0.5	1.5,2.2	1.4,2.1	1.2,1.7	0.7,0.5	2.0,3.4	1.8,3.0	1.4,1.5	0.7,0.8	0.7,0.8	
18	0.3,0.2	0.2,0.2	0.3,0.2	0.4,0.3	0.3,0.2	0.3,0.3	1.0,1.9	0.9,1.8	0.7,1.4	0.3,0.2	1.7,3.2	1.4,2.8	0.9,1.1	0.5,0.6	0.5,0.5	
19	0.4,0.3	0.4,0.3	0.4,0.3	0.7,0.4	0.4,0.3	0.6,0.4	1.4,2.2	1.2,2.1	1.0,1.7	0.5,0.4	2.0,3.5	1.7,3.1	1.2,1.3	0.7,0.7	0.6,0.6	
20	0.2,0.2	0.2,0.2	0.2,0.2	0.3,0.2	0.2,0.2	0.3,0.2	1.3,1.6	1.2,1.5	0.9,1.2	0.3,0.2	2.0,2.6	1.7,2.3	0.8,0.9	0.4,0.4	0.4,0.4	
21	0.2,0.1	0.2,0.1	0.2,0.1	0.2,0.2	0.2,0.1	0.2,0.2	0.7,2.1	0.6,2.0	0.5,1.5	0.2,0.2	1.4,4.2	1.1,3.5	0.6,0.9	0.4,0.3	0.3,0.3	
22	0.1,0.1	0.1,0.1	0.1,0.1	0.1,0.1	0.1,0.1	0.1,0.2	0.7,1.8	0.6,1.7	0.4,1.3	0.1,0.1	1.4,3.1	1.1,2.7	0.5,0.8	0.3,0.3	0.2,0.3	
23	0.4,0.3	0.3,0.3	0.4,0.3	0.6,0.4	0.4,0.3	0.6,0.4	1.7,2.1	1.6,2.0	1.3,1.6	0.6,0.4	2.4,3.3	2.1,3.0	1.2,1.2	0.6,0.6	0.5,0.5	
24	0.0,0.0	0.0,0.0	0.0,0.0	0.0,0.0	0.0,0.0	0.0,0.0	0.1,1.0	0.1,1.0	0.1,0.7	0.0,0.0	0.3,2.2	0.2,1.9	0.2,0.3	0.1,0.1	0.1,0.1	
25	0.4,0.3	0.4,0.3	0.4,0.3	0.7,0.5	0.4,0.3	0.7,0.4	1.6,3.1	1.4,2.9	1.2,2.2	0.6,0.4	2.5,5.2	2.1,4.7	1.5,2.0	0.8,1.0	0.8,1.0	
26	0.4,0.3	0.4,0.3	0.4,0.3	0.7,0.5	0.4,0.3	0.7,0.4	1.6,3.1	1.4,2.9	1.1,2.2	0.6,0.4	2.5,5.2	2.0,4.7	1.5,2.0	0.8,1.0	0.8,1.0	

geographic variations. Due to these large variations, it is difficult to provide typical V_d values from the model. We therefore ran the model for a wide, but realistic range of input values for these parameters, and estimated the typical range of V_d values and compared them with published measurements. Here we present the results for each LUC under dry and wet canopy conditions assuming a reference height for the V_d calculation of 20 m. The range of u_* values used depended upon the LUCs with the two roughest surfaces, evergreen and tropical broadleaf forests (LUC 5 and 8), being assigned values within the range of 0.1–1.5 m s⁻¹; forests and urban areas, a range of 0.1–1.2 m s⁻¹; and the remaining surfaces, a range of 0.1–0.8 m s⁻¹. These values were taken from available observation data (Meyers et al., 1998; Finkelstein et al., 2000). Surface temperature was allowed to vary between -10 and 30°C, solar radiation from 0 to 800 W m⁻² and relative humidity from 50–90%. All possible contributions of u_* , T , SR and RH were input separately into the model (using small increments for all variables: 0.1 for u_* , 1°C for T , 50 W m⁻² for SR and 5% for RH) to calculate the range of V_d values possible for each LUC. In addition, calculations were done for the first day of every month so that the seasonal variation of LAI was accounted for. Since, realistically, some of the test conditions would be highly unlikely (e.g. high temperatures and large solar radiation over tundra), the allowed ranges were adjusted so that 5°C is the minimum temperature for tropical forests and 20°C and 500 W m⁻² are the maximum values for tundra. We expect that the maximum V_d values (Table 2) extracted from these model test runs will be representative of the real-world typical maximum V_d , excluding some extreme conditions (e.g. ~1% largest values ever observed), for most land types under dry and wet conditions.

The maximum calculated V_d values for dry forest canopies and agricultural lands range around 0.9–1.7 cm s⁻¹ for SO₂, 0.6–1.5 cm s⁻¹ for O₃ and 3.3–5.3 cm s⁻¹ for HNO₃. NO₂ V_d follows the pattern of O₃ V_d but with slightly smaller values ($\alpha=0$, $\beta=0.8$). H₂O₂ V_d is higher than both SO₂ and O₃ during both day and night ($\alpha=1$, $\beta=1$). HNO₃ has the highest V_d among all the chemical species considered here due to its high solubility and reactivity ($\alpha=10$, $\beta=10$). The V_d of PAN mimics the pattern of O₃ ($\alpha=0$, $\beta=0.6$) but is always smaller while the V_d of HCHO follows the pattern of SO₂ ($\alpha=0.8$, $\beta=0.2$). NH₃ is similar to SO₂ ($\alpha=1$, $\beta=0$), but slightly higher during the day due to its higher molecular diffusivity (Note that bi-directional exchange for NH₃ is not treated in the present study). The V_d of ROOH is similar to the values for O₃ ($\alpha=0.1$, $\beta=0.8$). The V_d of H₂SO₄ and HNO₂ follows the pattern of HNO₃ but is smaller. Minimum V_d values (not presented in Table 2) for most chemical species are around 0.01–0.05 cm s⁻¹ for most LUCs. It could be even smaller if u_* were given smaller values (e.g. <0.1 m s⁻¹).

Maximum SO₂ (and other similar species) V_d values for wet canopies are much larger than for dry canopies due to

SO₂ solubility and reactivity. The increases are usually larger for canopies with larger LAI . Maximum O₃ (and other similar species) V_d values for wet canopies are very close to those for dry canopies, due to the two contradictory factors, the increase in cuticle uptake and the decrease in stomatal blocking (Zhang et al., 2002b).

As mentioned above, values in Table 2 do not cover the extreme conditions. If u_* is larger than values used above, V_d values can be larger than those presented in Table 2. For example, if a value of 1.5 m s⁻¹ instead of 1.2 m s⁻¹ was used for u_* over deciduous forests (LUC 6 and 7), maximum O₃ V_d values would be 2.0 cm s⁻¹ and 1.4 cm s⁻¹ for LUC 6 and 7, respectively. The larger u_* values are possible considering the large roughness length of forests. For example, of 2722 available u_* measurement samples at Kane site (deciduous forest) discussed in Sect. 4.1, 31 (~1% of total samples) have values larger than 1.2 m s⁻¹ and 6 have values larger than 1.5 m s⁻¹. Measured O₃ V_d for the same site has 5% larger than 1.2 cm s⁻¹ and 1% larger than 1.5 cm s⁻¹. It seems that the model can predict large enough O₃ V_d for needleleaf forests, even for extreme conditions compared to measurements (~2 cm s⁻¹). The model fails to predict extreme O₃ V_d for broadleaf forests (including tropical forest), unless even larger u_* values are used. This is caused by too large values chosen for two input parameters (R_{cutd0} and R_{cutw0}), which seems to work well if extreme conditions (~1%) are excluded. As discussed in Zhang et al. (2002), the model was developed using measurements that exclude (1 to 3%) extreme conditions.

Zhang et al. (2002a) reviewed and discussed all published measurements for all species of interest. Most flux measurements of SO₂, O₃, NO₂, NH₃ and HNO₃ support the results generated from the present model. The very limited set of measurements for PAN, HCHO, H₂O₂ and ROOH also agree well with model results. As indicated earlier, there are no data for the other species and thus Table 2 provides only a first-order estimation of their deposition rates, which cannot be validated at present stage.

4.3 Modelled typical V_d values under different dry and wet conditions

To attempt to provide an indication of the typical V_d values (instead of the maximum range as shown in Table 2) and to demonstrate the effect of day vs. night, wet vs. dry and snow conditions, we ran the model again using typical values for the input parameters. Table 3 lists the u_* values used for different LUCs for several typical conditions. Note that u_* for dry and rainy summer days was given the same set of values, as for dry and rainy summer night, while u_* for dewy summer nights was assumed smaller values. Typically LUC 5 (evergreen broadleaf trees) and 8 (tropical broadleaf trees) can expect to have the largest u_* values reflecting their large roughness; conversely, smooth surfaces (ice, water, tundra) have the smallest u_* values. The other dominant

Table 3. Friction velocity (m s^{-1}) used for producing Table 4.

LUC		Day dry or rain	Night dry or rain	Night dew	Day Snow
1	water	0.3	0.25	0.2	0.3
2	ice	0.25	0.15	0.15	0.25
3	inland lake	0.25	0.2	0.2	0.25
4	evergreen needleleaf trees	0.6	0.3	0.2	0.45
5	evergreen broadleaf trees	0.7	0.35	0.2	0.5
6	deciduous needleleaf trees	0.6	0.3	0.2	0.45
7	deciduous broadleaf trees	0.6	0.3	0.2	0.45
8	tropical broadleaf trees	0.7	0.35	0.2	0.5
9	drought deciduous trees	0.6	0.3	0.2	0.45
10	evergreen broadleaf shrubs	0.4	0.2	0.2	0.3
11	deciduous shrubs	0.4	0.2	0.2	0.3
12	thorn shrubs	0.4	0.2	0.2	0.3
13	short grass and forbs	0.4	0.2	0.2	0.3
14	long grass	0.4	0.2	0.2	0.3
15	crops	0.4	0.2	0.2	0.3
16	rice	0.4	0.2	0.2	0.3
17	sugar	0.4	0.2	0.2	0.3
18	maize	0.4	0.2	0.2	0.3
19	cotton	0.4	0.2	0.2	0.3
20	irrigated crops	0.4	0.2	0.2	0.3
21	urban	0.6	0.3	0.2	0.45
22	tundra	0.25	0.15	0.15	0.25
23	swamp	0.4	0.2	0.2	0.3
24	Desert	0.25	0.15	0.15	0.25
25	mixed wood forests	0.6	0.3	0.2	0.45
26	Transitional forest	0.6	0.3	0.2	0.45

meteorological variables used for the tests are: 20°C (T), 75% (RH) and 600 Wm^{-2} (SR) for dry summer day; 20°C (T) and 200 Wm^{-2} (SR) for rain summer day; 10°C (T) and 75% (RH) for dry summer night; and -2°C (T) and 20 cm (SD) for snow-covered conditions (note that for ice surfaces, the temperature is given a value of -2°C for all the tests). Only 5 chemical species are presented here (Table 4) as examples. Results for other species can be obtained by comparing their two scaling parameters (α and β in Zhang et al., 2002a) and by comparing their maximum V_d values in Table 2 with those of the 5 species shown.

For SO_2 and O_3 , V_d is found to typically be around $0.6\text{--}0.9\text{ cm s}^{-1}$ for a summer day for most vegetated surfaces with dry canopy conditions. As expected, V_d is larger over canopies with larger LAI (e.g. forests) and smaller r_{smin} (e.g. crops LUCs 15–17). Stomatal resistance is the dominant term during dry daytime conditions. When canopies are wet due to rain, SO_2 V_d increases substantially for vegetated surfaces due to increased cuticle uptake. During nighttime over dry canopies, SO_2 V_d is around $0.2\text{--}0.4\text{ cm s}^{-1}$, and O_3 V_d is $0.1\text{--}0.3\text{ cm s}^{-1}$. V_d of SO_2 is larger than that of O_3 due to the smaller cuticle and soil resistances assigned to SO_2 . During nighttime over wet canopies caused by rain,

V_d of O_3 is slightly larger compared to dry nighttime conditions, while V_d of SO_2 is substantially larger. The main result is that when canopies are wetted by dew, both SO_2 and O_3 have slightly larger V_d values compared to dry nighttime conditions assuming u_* values are the same. However, since u_* under dew conditions is usually smaller than under dry and rainy conditions (as was found in Zhang et al., 2003), V_d values under dew conditions are not necessarily larger than under dry conditions, as shown in Table 4. In winter when there is snow, SO_2 V_d is around 0.4 cm s^{-1} . However, it can be close to 1 cm s^{-1} over snow surfaces if the temperature is higher than 1°C (see Eq. 8a). O_3 V_d is less than 0.1 cm s^{-1} if the surfaces are fully covered by snow, but can be higher than 0.2 if the surfaces are partially covered by snow (e.g. forest canopies). It is well known that surface resistance (R_c) for HNO_3 is very small (i.e. $<20\text{ s m}^{-1}$). Thus, aerodynamic resistance (R_a) usually dominates the rate of HNO_3 dry deposition. However, R_c of HNO_3 can be substantially larger (e.g. $>100\text{ s m}^{-1}$) under very dry conditions (e.g. $RH < 20\%$, Tarnay et al., 2002). Many models specify a lower limit for R_c of HNO_3 (e.g. 10 s m^{-1} in Wesely, 1989 and Brook et al., 1999a). In the present study, we do not set a lower limit, but calculate R_c for HNO_3 using two

Table 4. Predicted dry deposition velocity (cm s^{-1}) for chemical species SO_2 , HCHO, O_3 , PAN and HNO_3 under 6 typical conditions: dry summer day, rain summer day, dry summer night, dew summer night, rain summer night and winter day with snow.

LUC	SO_2						HCHO						O_3						PAN						HNO_3										
	Dry Day	Rain Day	Dry Night	Dew Night	Rain Night	Snow Day	Dry Day	Rain Day	Dry Night	Dew Night	Rain Night	Snow Day	Dry Day	Rain Day	Dry Night	Dew Night	Rain Night	Snow Day	Dry Day	Rain Day	Dry Night	Dew Night	Rain Night	Snow Day	Dry Day	Rain Day	Dry Night	Dew Night	Rain Night	Snow Day	Dry Day	Rain Day	Dry Night	Dew Night	Rain Night
1	0.92	0.92	0.71	0.53	0.71	0.89	0.91	0.91	0.71	0.54	0.71	0.88	0.05	0.05	0.05	0.05	0.05	0.05	0.03	0.03	0.03	0.03	0.03	0.03	1.01	1.01	0.76	0.56	0.76	0.97					
2	0.55	0.55	0.39	0.36	0.39	0.55	0.5	0.5	0.37	0.35	0.37	0.5	0.05	0.05	0.05	0.05	0.05	0.05	0.03	0.03	0.03	0.03	0.03	0.03	1.1	1.1	0.61	0.54	0.61	1.08					
3	0.79	0.79	0.58	0.53	0.58	0.76	0.79	0.79	0.59	0.54	0.59	0.76	0.05	0.05	0.05	0.05	0.05	0.05	0.03	0.03	0.03	0.03	0.03	0.03	0.86	0.86	0.62	0.56	0.62	0.82					
4	0.84	1.94	0.24	0.35	0.87	0.36	0.95	1.88	0.22	0.34	0.82	0.35	0.73	0.91	0.15	0.21	0.34	0.23	0.51	0.62	0.11	0.14	0.23	0.17	2.97	3.39	1.35	1.17	1.88	1.96					
5	0.88	2.47	0.22	0.38	1.12	0.29	1.01	2.36	0.2	0.35	1.03	0.26	0.74	0.79	0.11	0.12	0.23	0.15	0.51	0.53	0.08	0.08	0.15	0.11	3.34	4.07	1.53	1.31	2.39	2.03					
6	0.84	1.94	0.24	0.35	0.87	0.33	0.94	1.88	0.22	0.33	0.81	0.32	0.73	0.91	0.15	0.21	0.33	0.25	0.51	0.62	0.11	0.14	0.22	0.17	2.96	3.39	1.35	1.17	1.88	1.35					
7	0.8	1.92	0.18	0.35	0.86	0.27	0.93	1.84	0.16	0.31	0.79	0.26	0.71	0.66	0.09	0.11	0.18	0.2	0.49	0.45	0.06	0.07	0.12	0.14	2.66	3.42	1.2	1.14	1.91	1.15					
8	0.87	2.5	0.22	0.39	1.14	0.28	1	2.38	0.2	0.35	1.04	0.26	0.73	0.78	0.11	0.12	0.22	0.14	0.51	0.52	0.07	0.08	0.15	0.1	3.41	4.18	1.56	1.36	2.48	2.06					
9	0.48	1.77	0.11	0.32	0.8	0.19	0.57	1.68	0.11	0.29	0.73	0.19	0.51	0.59	0.1	0.12	0.19	0.15	0.36	0.41	0.08	0.08	0.13	0.12	1.79	3.25	0.79	1.04	1.78	1.21					
10	0.63	1.1	0.3	0.29	0.46	0.28	0.73	1.08	0.27	0.27	0.42	0.25	0.57	0.5	0.12	0.12	0.12	0.1	0.41	0.36	0.09	0.09	0.09	0.07	1.62	2.15	0.96	0.88	1.06	1.2					
11	0.71	1.12	0.3	0.29	0.46	0.35	0.84	1.12	0.27	0.27	0.42	0.32	0.68	0.6	0.14	0.14	0.14	0.15	0.49	0.43	0.1	0.1	0.1	0.09	1.67	2.15	0.97	0.89	1.06	1.08					
12	0.57	1.09	0.31	0.3	0.47	0.3	0.63	1.06	0.29	0.28	0.44	0.27	0.5	0.5	0.16	0.16	0.16	0.12	0.36	0.35	0.12	0.12	0.12	0.08	1.64	2.15	0.97	0.89	1.07	1.22					
13	0.64	0.9	0.27	0.26	0.37	0.42	0.66	0.89	0.26	0.25	0.35	0.38	0.5	0.51	0.2	0.19	0.2	0.09	0.36	0.36	0.15	0.15	0.15	0.06	1.62	1.85	0.76	0.7	0.84	1.22					
14	0.74	0.97	0.27	0.26	0.37	0.45	0.81	0.99	0.26	0.25	0.35	0.4	0.63	0.63	0.2	0.19	0.2	0.09	0.46	0.45	0.15	0.15	0.15	0.06	1.65	1.87	0.77	0.7	0.85	1.18					
15	0.8	1.12	0.31	0.3	0.45	0.46	0.91	1.14	0.3	0.29	0.43	0.41	0.75	0.71	0.21	0.2	0.21	0.09	0.55	0.51	0.15	0.15	0.15	0.06	1.7	1.96	0.9	0.82	0.97	1.2					
16	0.89	1.19	0.33	0.32	0.48	0.46	1.01	1.21	0.32	0.31	0.46	0.41	0.8	0.76	0.22	0.22	0.22	0.09	0.59	0.55	0.16	0.16	0.16	0.06	1.73	1.95	0.91	0.83	0.97	1.2					
17	0.79	1.18	0.33	0.32	0.49	0.46	0.93	1.2	0.32	0.31	0.46	0.41	0.78	0.74	0.22	0.21	0.22	0.09	0.58	0.53	0.16	0.15	0.16	0.06	1.65	1.97	0.93	0.84	0.99	1.2					
18	0.54	1.03	0.3	0.29	0.45	0.46	0.6	1	0.28	0.27	0.42	0.41	0.47	0.47	0.16	0.15	0.16	0.09	0.34	0.34	0.12	0.11	0.12	0.06	1.52	1.96	0.88	0.8	0.96	1.2					
19	0.67	1.18	0.34	0.33	0.5	0.46	0.77	1.16	0.32	0.31	0.47	0.41	0.62	0.58	0.18	0.17	0.18	0.09	0.45	0.41	0.13	0.13	0.13	0.06	1.68	2.11	0.98	0.89	1.06	1.2					
20	0.7	0.93	0.27	0.26	0.37	0.42	0.74	0.92	0.26	0.25	0.35	0.38	0.44	0.45	0.17	0.17	0.17	0.09	0.3	0.3	0.12	0.12	0.12	0.06	1.45	1.88	0.78	0.71	0.86	1.24					
21	0.5	1.41	0.19	0.24	0.6	0.38	0.54	1.33	0.18	0.22	0.55	0.34	0.42	0.41	0.14	0.11	0.17	0.1	0.27	0.27	0.1	0.08	0.12	0.06	2.03	3.43	0.88	0.93	1.77	1.63					
22	0.31	0.84	0.43	0.4	0.54	0.47	0.29	0.8	0.41	0.38	0.53	0.43	0.19	0.2	0.17	0.16	0.17	0.1	0.12	0.13	0.11	0.11	0.11	0.06	1.12	1.21	0.68	0.61	0.68	1.16					
23	0.91	1.23	0.36	0.34	0.51	0.41	1.01	1.23	0.34	0.33	0.48	0.37	0.71	0.63	0.18	0.18	0.18	0.09	0.5	0.43	0.13	0.13	0.13	0.06	1.76	2.01	0.93	0.85	1	1.3					
24	0.13	0.83	0.43	0.4	0.55	0.47	0.14	0.79	0.41	0.38	0.54	0.42	0.18	0.18	0.16	0.16	0.16	0.09	0.11	0.11	0.1	0.1	0.1	0.06	1	1.24	0.7	0.63	0.7	1.19					
25	0.91	1.98	0.2	0.35	0.87	0.3	1.08	1.95	0.2	0.34	0.82	0.29	0.89	0.99	0.15	0.21	0.34	0.21	0.62	0.68	0.11	0.14	0.23	0.15	2.84	3.39	1.27	1.17	1.88	1.69					
26	0.88	1.97	0.2	0.35	0.87	0.29	1.04	1.94	0.2	0.34	0.82	0.27	0.85	0.97	0.15	0.21	0.34	0.2	0.6	0.66	0.11	0.14	0.23	0.15	2.83	3.39	1.27	1.17	1.88	1.69					

scaling parameters ($\alpha=10$, $\beta=10$). For summer daytime dry canopy conditions, V_d of HNO_3 is higher than 1.5 cm s^{-1} for canopies with small roughness lengths and higher than 3 cm s^{-1} for forest canopies with larger roughness lengths. Under wet conditions, V_d values are even larger. This is because R_a is small (e.g. $<20 \text{ s m}^{-1}$) under unstable stratification conditions and is in the same magnitude as R_c . Thus, decreases in R_c under rain conditions will increase V_d . During the nighttime, HNO_3 V_d is still close to 1.0 cm s^{-1} for canopies with small z_0 values and even higher for canopies with large z_0 . HNO_3 V_d under dry nighttime conditions is slightly larger than under rainy nighttime conditions, but V_d under dew conditions is close (slightly smaller or larger) to that under dry conditions, mainly due to the dominant role of aerodynamic resistance under stable conditions. As discussed earlier, and also shown in Table 4, V_d of HCHO follows the pattern of SO_2 and V_d of PAN mimics the pattern of O_3 . Overall, the typical V_d values shown in Table 4 are consistent with the published measurements reviewed by Sehmel (1984), Brook et al. (1999b), Wesely and Hicks (2000) and Zhang et al. (2002a). Again, for many

species that do not have measurements, the tables presented here are believed to provide some useful information for applications where deposition velocities are needed.

5 Conclusions and recommendations

A revised parameterization for estimating dry deposition velocities in air-quality models that includes a newly developed non-stomatal resistance formulation, a realistic treatment of cuticle and ground resistance in winter (low temperature and snow-covered surfaces) and the handling of seasonally-dependent input parameters (i.e. LAI , z_0 , resistance components) has been found to predict more realistic deposition velocities compared to other existing models, especially for wet canopies. Modelled maximum deposition velocities derived from values of typical meteorological conditions are also found to be realistic compared to published measurements. However, there are few measurements of V_d for chemical compounds other than SO_2 , O_3 , NO_2 , HNO_3 , NH_3 . Hence, although the approach presented here is expected to be reasonably realistic for those other compounds,

Table 5. Appendix A: Nomenclature.

α :	parameter for cuticle and soil resistances scaling to SO ₂ (0.0–10.0)
β :	parameter for cuticle and soil resistances scaling to O ₃ (0.0–10.0)
$\psi, \psi_{c1}, \psi_{c2}$:	leaf-water-potential (Mpa)
b_{rs} :	empirical light response constant for stomatal resistance (W m ⁻²)
b_{vpd} :	water-vapour-pressure-deficit constant (kPa ⁻¹),
D :	vapour pressure deficit (kPa),
e, e^* :	ambient and saturation water vapour pressure (kPa), respectively.
f_{snow} :	snow cover fraction (0.0–1.0)
LAI :	leaf area index (m ² m ⁻²)
r_{smin} :	minimum stomatal resistance (s m ⁻¹)
R_a :	aerodynamic resistance (s m ⁻¹). Same unit for all resistance parameters listed below.
R_{ac}, R_{ac0} :	in-canopy aerodynamic resistance
R_b :	quasi-laminar sublayer resistance
R_c :	canopy resistance
R_{cut} :	cuticle resistance
R_{cutd}, R_{cutd0} :	dry cuticle resistance
R_{cutw}, R_{cutw0} :	wet cuticle resistance
R_g :	ground resistance
R_{gdew}, R_{grain} :	soil resistance with dew and rain, respectively
R_{ice} :	ice resistance
R_m :	mesophyll resistance
R_{ns} :	non-stomatal resistance
R_{snow} :	snow resistance
R_{soil} :	soil resistance
R_{st} :	stomatal resistance
R_{water} :	water resistance
RH :	relative humidity (0–100%)
sd, sd_{max} :	snow depth (cm)
SR :	solar radiation (W m ⁻²)
$T_{min}, T_{max}, T_{opt}$:	minimum, maximum and optimum temperature for stomatal opening (°C), respectively.
u_* :	friction velocity (m s ⁻¹)
V_d :	dry deposition velocity (m s ⁻¹)
W_{st} :	fraction of stomatal blocking (0.0–0.5)
z_0 :	roughness length (m)

many of the estimated values presented in this paper have not been validated due to the lack of data.

Though the model performs better compared to its earlier version, it clearly still has limitations and uncertainties as discussed in the Introduction. To improve future dry deposition models further evaluations are needed using data from many different sites, especially sites not used for model development. Unfortunately, flux measurements in many locations where dry deposition may be important (e.g. rough terrain, “edges” or step changes in vegetation/land-use) are not possible, though there exist some limited theoretical studies (Physick and Garratt, 1995; De Jong and Klaassen, 1997). Yet air quality models are required to include deposition in such situations. Also, measurements of SO₂ deposition over different wetness conditions are needed in order to verify the assumptions made in the present study; and simultaneous flux measurements of CO₂, H₂O and pollutant gaseous species (e.g. O₃, SO₂) are needed to verify the assumption

that stomatal uptake is not important under wet conditions. It is important to include the compensation point of NH₃ for areas where NH₃ emission can occur. However, all the information necessary to implement this formulation in regional scale models and/or across multiple locations is not available.

Many chemical species are estimated to have high deposition velocities, yet these have never been measured. Any measurement of flux for these species would be valuable to be able to begin verifying the scaling method. This is probably difficult to measure for species with very low concentrations since no instruments exist with suitable sensitivity and fast enough response time. However, there are approaches for dealing with the fluxes of chemically reactive species, as long as their concentrations are high enough for the measurement techniques. Even soil resistance to different gaseous species over different surfaces (e.g., snow, ice, bare soil, below canopy) needs further investigation. Separate measurements of stomatal and non-stomatal uptake are

Table 6. Appendix B: Definition of 31 species.

No.	Symbol	Name
1	SO ₂	Sulphur dioxide
2	H ₂ SO ₄	Sulphuric acid
3	NO ₂	Nitrogen dioxide
4	O ₃	Ozone
5	H ₂ O ₂	Hydrogen peroxide
6	HNO ₃	Nitric acid
7	HONO	Nitrous acid
8	HNO ₄	Pernitric acid
9	NH ₃	Ammonia
10	PAN	Peroxyacetylnitrate
11	PPN	Peroxypropylnitrate
12	APAN	Aromatic acylnitrate
13	MPAN	Peroxymethacrylic nitric anhydride
14	HCHO	Formaldehyde
15	MCHO	Acetaldehyde
16	PALD	C3 Carbonyls
17	C4A	C4-C5 Carbonyls
18	C7A	C6-C8 Carbonyls
19	ACHO	Aromatic carbonyls
20	MVK	Methyl-vinyl-ketone
21	MACR	Methacrolein
22	MGLY	Methylglyoxal
23	MOH	Methyl alcohol
24	ETOH	Ethyl alcohol
25	POH	C3 alcohol
26	CRES	Cresol
27	FORM	Formic acid
28	ACAC	Acetic acid
29	ROOH	Organic peroxides
30	ONIT	Organic nitrates
31	INIT	Isoprene nitrate

also important for evaluating the stomatal uptake sub-model for the purpose of estimating O₃ damage to crops (Ashmore and Fuhrer, 2000; Emberson et al. 2000) and to develop a broader understanding of the relative importance of these two pathways. Clearly, further model developments, beyond what is presented in this paper, relies heavily on the availability of more extensive and detailed measurements in the future.

Acknowledgements. We greatly appreciate S. Belair and J. St-James of the Canadian Meteorological Center in Montreal for providing GEM related information, M. D. Moran, P. A. Makar, R. Staebler and several AURAMS group members of the Meteorological Service of Canada for helpful comments and P. L. Finkelstein of USEPA for sharing measurement data. Constructive comments from three anonymous reviewers are also appreciated.

References

Ashmore, M. and Fuhrer, J.: New Directions: Use and abuse of the AOT40 concept, *Atmos. Environ.*, 34, 1157–1158, 2000.

- Baldocchi, D. D.: A multi-layer model for estimating sulfur dioxide deposition to a deciduous oak forest canopy, *Atmos. Environ.*, 22, 869–884, 1988.
- Baldocchi, D. D., Hicks, B. B., and Camara, P.: A canopy stomatal resistance model for gaseous deposition to vegetated surfaces, *Atmos. Environ.*, 21, 91–101, 1987.
- Brook, J., Zhang, L., Franco, D., and Padro, J.: Description and evaluation of a model of deposition velocities for routine estimates of air pollutant dry deposition over North America, Part I: Model development, *Atmos. Environ.*, 33, 5037–5052, 1999a.
- Brook, J., Zhang, L., Franco, D., and Padro, J.: Description and evaluation of a model of deposition velocities for routine estimates of air pollutant dry deposition over North America, Part II: Review of past measurements and model results, *Atmos. Environ.*, 33, 5053–5070, 1999b.
- Byun, D. W. and Ching, J. K. S.: Science Algorithms of the EPA Models-3 Community Multiscale Air Quality (CMAQ) Modeling System, EPA/600/R-99/030, Environmental Protection Agency, Office of Research and Development, Washington, DC, 1999.
- Carmichael, G. R., Peters, L. K., and Saylor, R. D.: The STEM-II regional scale acid deposition and photochemical oxidant model, 1: An overview of model development and applications, *Atmos. Environ.*, 25, 2077–2090, 1991.
- Chameides, W. L.: Acid dew and the role of chemistry in the dry deposition of reactive gases to wetted surfaces, *J. Geophys. Res.*, 92, 11 895–11 900, 1987.
- Chang, J. S., Brost, R. A., Isaksen, I. S. A., Madronich, S., Middleton, P., Stockwell, W. R., and Walcek, C. J.: A three-dimensional Eulerian acid deposition model: Physical concepts and formulation, *J. Geophys. Res.*, 92, 14 681–14 700, 1987.
- Coté, J., Desmarais, J. G., Gravel, S., Methot, A., Patoine, A., Roch, M., and Staniforth, A.: The operational CMC/MRB global environmental multiscale (GEM) model, Part I, design considerations and formulation, *Mon. Wea. Rev.*, 126, 1373–1395, 1997.
- De Jong, J. J. M. and Klaassen, W.: Simulated dry deposition of nitric acid near forest edges, *Atmos. Environ.*, 31, 3681–3691, 1997.
- Dickinson, R. E., Henderson-Sellers, A., Kennedy, P. J., and Wilson, M. F.: Biosphere-Atmosphere Transfer Scheme (BATS) for the NCAR Community Climate Model. NCAR Technical Note NCAR/TN275+STR, National Centre for Atmospheric Research, Boulder, Colorado, 67, 1986.
- Dorman, J. L. and Sellers, P. J.: A global climatology of albedo, roughness length and stomatal resistance for atmospheric general circulation models as represented by the simple biosphere model (SiB), *J. Appl. Meteor.*, 28, 833–855, 1989.
- Duyzer, J. and Fowler, D.: Modelling land atmosphere exchange of gaseous oxides of nitrogen in Europe, *Tellus, Chemical and Physical Meteorology*, 46B, 353–372, 1994.
- Emberson, L. D., Ashmore, M. R., Cambridge, H. M., Simpson, D., and Tuovinen, J. P.: Modelling stomatal ozone flux across Europe, *Environ. Pollu.*, 109, 403–413, 2000.
- Erisman, J. W. and Wyers, G. P.: Continuous measurements of surface exchange of SO₂ and NH₃: implications for their possible interaction in the deposition process, *Atmos. Environ.*, 27, 1937–1949, 1993.
- Erisman, J. W., van Elzakker, B. G., Mennen, M. G., Hogenkamp, J., Zwart, E., van den Beld, L., Römer, F. G., Bobbink, R., Heil,

- G., Raessen, M., Duyzer, J. H., Verhage, H., Wyers, G. P., Ojjes, R. P., and Mols, J. J.: The Elspeetsche Veld experiment on surface exchange of trace gases: Summary of results, *Atmos. Environ.*, 28, 487–496, 1994a.
- Erismann, J. W., Van Pul, A., and Wyers, G. P.: Parameterization of surface resistance for the quantification of atmospheric deposition of acidifying pollutants and ozone, *Atmos. Environ.*, 28, 2595–2607, 1994b.
- Finkelstein, P. L., Ellestad, T. G., Clarke, J. F., Meyers, T. P., Schwede, D., Hebert, E. O., and Neal, J. F.: Ozone and sulfur dioxide dry deposition to forests: observations and model evaluation, *J. Geophys. Res.*, 105, 15 365–15 377, 2000.
- Flechar, C. R., Fowler, D., Sutton, M. A., and Cape, J. N.: A dynamic chemical model of bi-directional ammonia exchange between semi-natural vegetation and the atmosphere, *Q. J. R. Meteorol. Soc.*, 125, 2611–2641, 1999.
- Fowler, D. and Unsworth, M. H.: Turbulent transfer of sulphur dioxide to a wheat crop. *Quarterly J. Royal Meteorol. Soc.*, 105, 767–783, 1979.
- Fuentes, J. D., Gillespie, T. J., den Hartog, G., and Neumann, H. H.: Ozone deposition onto a deciduous forest during dry and wet conditions, *Agricultural forest meteorology* 62, 1–18, 1992.
- Ganzeveld, L. and Lelieveld, J.: Dry deposition parameterization in a chemistry general circulation model and its influence on the distribution of reactive trace gases, *J. Geophys. Res.*, 100, 20 999–21 012, 1995.
- Gao, W., Wesely, M. L., and Doskey, P. V.: Numerical modeling of the turbulent diffusion and chemistry of NO_x, O₃, isoprene, and other reactive trace gases in and above a forest canopy, *J. Geophys. Res.*, 98, 18 339–18 353, 1993.
- Grantz, D. A., Zhang, X. J., Massman, W. J., Den Hartog, G., Neumann, H. H., and Pederson, J. R.: Effects of stomatal conductance and surface wetness on ozone deposition in field-grown grape, *Atmos. Environ.*, 29, 3189–3198, 1995.
- Gunthardt-Goerg, M. S., McQuattie, C. J., Scheidegger, C., Rhiner, C., and Matyssek, R.: Ozone-induced cytochemical and ultrastructural changes in leaf mesophyll cell walls, *Canadian J. Forest Res.*, 27, 453–463, 1997.
- Harley, R. A., Russell, A. G., McRae, G. J., Cass, G. R., and Seinfeld, J. H.: Photochemical modeling of the Southern California Air Quality Study, *Environ. Sci. Tech.*, 27, 378–388, 1993.
- Hicks, B. B., Baldocchi, D. D., Meyers, T. P., Hosker Jr., R. P., and Matt, D. R.: A preliminary multiple resistance routine for deriving dry deposition velocities from measured quantities, *Water, Air and Soil Pollut.*, 36, 311–330, 1987.
- Hicks, B. B. and Liss, P. S.: Transfer of SO₂ and other reactive gases across the air-sea interface, *Tellus* 28, 348–354, 1976.
- Husted, S., Schjoerring, J. K., Nielsen, K. H., Nemitz, E., and Sutton, M. A.: Stomatal compensation points for ammonia in oilseed rape plants under field conditions, *Agri. For. Meteorol.*, 105, 371–383, 2000.
- Janssen, L. H. J. M. and Romer, F. G.: The frequency and duration of dew occurrence over a year, *Tellus*, 43B, 408–419, 1991.
- Jarvis, P. G.: The interpretation of the variations in leaf water potential and stomatal conductance found in canopies in the field, *Phil. Trans. R. Soc. London Ser. B*, 273, 593–610, 1976.
- Kramm, G., Dlugi, R., Dollard, G. J., Foken, T., Moelders, N., Mueller, H., Seiler, W., and Sievering H.: On the dry deposition of ozone and reactive nitrogen species, *Atmos. Environ.* 29, 3209–3231, 1995.
- Lamaud, E., Carrara, A., Brunet, Y., Lopez, A., and Druilhet, A.: Ozone fluxes above and within a pine forest canopy in dry and wet conditions, *Atmos. Environ.*, 36, 77–88, 2002.
- Laville, P., Cellier, P., Lamaud, E., and Lopez, A.: Micrometeorological measurements of ozone fluxes on a maize crop during the ESCOMPTE experiment, Presented at Joint International Symposium on Atmospheric Chemistry within the Earth System, 18–25 September 2002, Crete, Greece, Abstract and Poster, 2002.
- Lopez, A., Bouchou, P., Brustet, J. M., and Fontian, J.: Ozone vertical fluxes at the interface vegetation-atmosphere, Presented at Joint International Symposium on Atmospheric Chemistry within the Earth System, 18–25 September 2002, Crete, Greece, Abstract and Poster, 2002.
- Massman, W. J., Musselman, R. C., and Lefohn, A. S.: A conceptual ozone dose-response model to develop a standard to protect vegetation, *Atmos. Environ.*, 34, 745–759, 2000.
- Massman, W. J., Pederson, J., Delany, A., Grantz, D., den Hartog, G., Neumann, H. H., Oncley, S. P., Pearson, R., and Shaw, R. H.: An evaluation of the Regional Acid Deposition Model surface module for ozone uptake at three sites in the San Joaquin Valley of California, *J. Geophys. Res.*, 99, 8281–8294, 1994.
- Meyers, T. P., Finkelstein, P. L., Clarke, J., Ellestad, T. G., and Sims, P. F.: A multi-layer model for inferring dry deposition using standard meteorological measurements, *J. Geophys. Res.*, 103, 22 645–22 661, 1998.
- McDonald-Buller, E. C., Liljestrang, H. M., and Sepehrnoori, K.: Numerical modeling of dry deposition coupled to 22 photochemical reactions, *Atmos. Environ.*, 33, 1491–1502, 1999.
- Moran, M. D., Dastoor, A., Gong, S. L., Gong, W., and Makar, P. A.: Proposed conceptual design for the AES regional particulate-matter model/unified model, Unpublished report, Meteorological Service of Canada, Downsview, Ontario, Canada, 1998.
- Musselman, R. C. and Minnick, T. J.: Nocturnal stomatal conductance and ambient air quality standards for ozone, *Atmos. Environ.*, 34, 719–733, 2000.
- NOAA: NOAA library of input data for “Bigleaf” and “Multi-layer” models, ATDD, NOAA, Oak Ridge, TN, 1992.
- Padro, J.: Summary of ozone dry deposition velocity measurements and model estimates over vineyard, cotton, grass and deciduous forest in summer, *Atmos. Environ.*, 30, 2363–2369, 1996.
- Padro, J., den Hartog, G., and Neumann, H. H.: An investigation of the ADOM dry deposition module using summertime O₃ measurements above a deciduous forest, *Atmos. Environ.*, 25, 1689–1704, 1991.
- Panofsky, H. A. and Dutton, J. A.: *Atmospheric Turbulence, Models and Methods for Engineering Applications*, John Wiley, New York, 1984.
- Physick, W. L. and Garratt, J. R.: Incorporation of a high-roughness lower boundary into a mesoscale model for studies of dry deposition over complex terrain, *Boundary-Layer Meteorol.*, 74, 55–71, 1995.
- Pielke, R. A.: *Mesoscale Meteorological Modelling*, Academic Press, New York, 1984.
- Pleim, J. E. and Xiu, A.: Development and testing of a surface flux and planetary boundary layer model for application in mesoscale models, *J. Appl. Meteorol.*, 34, 16–32, 1995.
- Sehmel, G. A.: Deposition and resuspension, In *Atmospheric science and power production*, edited by Randerson, D., NTIS,

- Springfield, VA, 533–583, 1984.
- Scire, J. S.: A review of the UAM-V dry deposition algorithm and recommendations for dry deposition modeling in the LMOS study region, Sigma Research Corporation, Westford, MA (Document A195-100), 1991.
- Sellers, P. J., Randall, D. A., Collatz, J. G., Berry, J. A., Field, C. B., Dazlich, D. A., Collelo, G. D., and Bounoua, L.: A revised land surface parameterization (SiB2) for atmospheric GCMs, Part I: Model formulation, *J. of Climate*, 9, 676–705, 1996.
- Singles, R., Sutton, M. A., and Weston, K. J.: A multi-layer model to describe the atmospheric transport and deposition of ammonia in Great Britain, *Atmos. Environ.*, 32, 393–399, 1998.
- Smith, R. I., Fowler, D., Sutton, M. A., Flechard, C., and Coyle, M.: Regional estimation of pollutant gas dry deposition in the UK: Model description, sensitivity analyses and outputs, *Atmos. Environ.*, 34, 3757–3777, 2000.
- Sorteberg, A. and Hov, O.: Two parametrizations of the dry deposition exchange for SO₂ and NH₃ in a numerical model, *Atmos. Environ.*, 30, 1823–1840, 1996.
- Sutton, M. A., Burkhardt, J. K., Guerin, D., Nemitz, E., and Fowler, D.: Development of resistance models to describe measurements of bi-directional ammonia surface atmospheric exchange, *Atmos. Environ.*, 32, 473–480, 1998.
- Tarnay, L. W., Gertler, A., Taylor Jr., G. E.: The use of inferential models for estimating nitric acid vapor deposition to semi-arid coniferous forests, *Atmos. Environ.*, 36, 3277–3287, 2002.
- Tetzlaff, G., Dlugi, R., Friedrich, K., Gross, G., Hinneburg, D., Pahl, U., Zelger, M., and Moelders, N.: On modeling dry deposition of long-lived and chemically reactive species over heterogeneous terrain, *J. Atmos. Chem.*, 42, 123–155, 2002.
- Wesely, M. L.: Parameterization of surface resistances to gaseous dry deposition in regional-scale numerical models, *Atmos. Environ.*, 23, 1293–1304, 1989.
- Wesely, M. L., Sisterson, D. L., and Jastrow, J. D.: Observations of the chemical properties of dew on vegetation that affect the dry deposition of SO₂, *J. Geophys. Res.*, 95, 7501–7514, 1990.
- Wesely, M. L. and Hicks, B. B.: A review of the current status of knowledge in dry deposition, *Atmos. Environ.*, 34, 2261–2282, 2000.
- Wesely, M. L., Doskey, P. V., and Shannon, J. D.: Deposition Parameterizations for the Industrial Source Complex (ISC3) Model, report to U.S. EPA, Argonne National Laboratory, USA, 2001.
- Wiser, G. and Havranek, W. M.: Ozone uptake in the sun and shade crown of spruce: quantifying the physiological effects of ozone exposure, *Trees*, 7, 227–232, 1993.
- Wiser, G. and Havranek, W. M.: Environmental control of ozone uptake in *Larix decidua* Mill: a comparison between different altitudes, *Tree Physiology*, 15, 253–258, 1995.
- Wu, Y., Brashers, B., Finkelstein, P. L., and Pleim, J. E.: A multi-layer biochemical dry deposition model, 1. Model formulation, *J. Geophys. Res.*, 108 D1, 4013, doi:10.1029/2002JD002293, 2003.
- Zhang, L., Moran, M., Makar, P., Brook, J., and Gong, S.: Modelling Gaseous Dry Deposition in AURAMS A Unified Regional Air-quality Modelling System, *Atmos. Environ.*, 36, 537–560, 2002a.
- Zhang, L., Brook, J., and Vet, R.: On Ozone dry deposition With emphasis on non-stomatal uptake and wet canopies, *Atmos. Environ.*, 36, 4787–4799, 2002b.
- Zhang, L., Brook, J., and Vet, R.: Evaluation of a non-stomatal resistance parameterization for SO₂ dry deposition, *Atmos. Environ.*, 37, 2941–2947, 2003.